MODELLING AND SIMULATION OF NITROGEN INJECTION IN VEGETABLE OLIVE OIL

Filippo Ferrari[(a)], Simone Spanu[(b)], Giuseppe Vignali[(c)]

[(a), (c)] Department of Industrial Engineering, University of Parma, Parco Area delle Scienze 181/A, 43124 Parma (Italy)
[(b)]CERIT Center, University of Parma, Parco Area delle Scienze 181/A, 43124 Parma (Italy)

[(a)]filippo.ferrari5@studenti.unipr.it, [(b)]simone.spanu@nemo.unipr.it, [(c)]giuseppe.vignali@unipr.it

ABSTRACT

The aim of this work is to analyze, by means of a CFD analysis, the injection of gaseous Nitrogen (N_2) in vegetable oil.

This process, called sparging, is important to enhance oil shelf-life, because it allows to separate by stripping the Oxygen (O_2) dissolved in the product. In fact, when the tank filling begins, N_2 bubbles start to rise towards the free surface of the product, dragging along with themselves part of the dissolved O_2. In this way the probability of initiation of oxidative reactions is reduced and, consequently, is reduced also the possibility of oil degradation.

The final goal of this work is to compare different sparger configurations and observe how they influence the stripping process during the tank filling phase.

The various configurations have been compared in terms of O_2 residual inside the tank at the end of the filling phase. The simulations still need to be experimentally validated.

Keywords: CFD, Vegetable Oil, Modified Atmosphere, Gas Flushing

1. INTRODUCTION

In the vegetable oils sector, keeping under control the aging process of the product is of particular importance to, because it can significantly influence the final quality of the sale unit. In fact, during aging, vegetable oils are subject to a process of degradation due to fats rancidity. This phenomenon affects the organoleptic characteristics of the product, but not its hygienic stability, as the vegetable oils have a very low water activity (a_w) and are hardly subject to microbial growth (Gunstone, 2011). For these reasons, no aseptic conditions must be maintained and only a clean filling technology is required. For the same reasons and due to the low resistance to the high temperatures, hot-filling technology is not admitted (Manfredi and Vignali, 2015)

One of the process phases that contributes more to the product degradation is storage. In this case, fats rancidity is mainly due to four factors (Choe and Min, 2006):

1. exposure to high conservation temperature (usually the maximum storage temperature is of 25°C, except for palm oil, which tends to solidify at room temperature (Shahidi, 2005));
2. exposure to light: low wavelength radiation (and thus high energy radiation) increase the probability of fat rancidity;
3. time: higher is the storage period higher will be the probability of fats rancidity;
4. exposure to Oxygen (O_2), since rancidity is due to the formation of free radicals and to the absorption of O_2 by fatty acids, especially unsaturated ones.

The first three factors are easily controlled: to avoid exposure to light and to high temperature is sufficient to keep the product in thermo-stated stainless steel tanks, while to avoid an excessively long storage period is sufficient a proper management of the oil purchasing process.

In order to minimize exposure to O_2, instead, three main techniques are adopted: minimization of tank head space, blanketing and sparging.

In the first case, when oil level has decreased under a certain limit, the product is moved to a lower-capacity tank, in order to keep head space minimized, and so on until stock exhaustion. When blanketing is applied, instead, the tank head space is filled with gaseous Nitrogen (N_2), or with a different inert gas, so to avoid the contact between oil and atmospheric O_2 during the entire period of storage. Finally, sparging process consists in injecting gaseous N_2 in the vegetable oil stream, thus, in this case, N_2 is directly mixed to the product. The goal of this treatment is to supersaturate vegetable oil with N_2. In this way, when the product starts to fill the tank, the previously injected gas is released through the oil free surface, pushing out the air and occupying the tank headspace. In some cases, blanketing and sparing are adopted simultaneously, saturating the tank with N_2 before the beginning of the tank filling phase, so to avoid the contact between oil and O_2 also during filling (Shahidi, 2005).

Compared to blanketing, sparging process has more advantages. When, during the tank filling phase, N_2 bubbles start to rise towards the free surface, they drag along with themselves part of the O_2 dissolved in the product (Masella et al., 2010). This contributes in reducing the vegetable oil alteration since, usually, there

can be a maximum of 36 mg/l of dissolved O_2 in the product (Parenti et al., 2007.).

As already proposed in other food sectors, in the case the process is hardly visible and experimental tests do not give sufficient information, a Computational Fluid Dynamics (CFD) approach can be used. As already shown in other works using multiphase flows (Spanu and Vignali, in press; Mosna and Vignali, 2015; Bottani et al, 2014), the advantages of using CFD are consistent and very affordable.

Based on these premises, the aim of this work is to adopt Computational Fluid Dynamics (CFD) to assess the efficacy of the N_2 sparging process in removing the O_2 dissolved in the oil. In particular, some different geometrical configuration of the duct in which is inserted the sparger will be analyzed, to check how a different geometry can influence the distribution of N_2 within the vegetable oil flow and, consequently, the removal of dissolved O_2.

2. MATERIALS AND METHODS

The sparging process that has been taken into account relies on a sparger (realized by *Mott Corp.*®) made of sintered stainless steel, with a porosity of about 70% and a nominal pore diameter of 40 μm.

2.1. Equipment

The way adopted to place the sparger inside the pipeline in which the vegetable oil flows is shown in Figure 1.

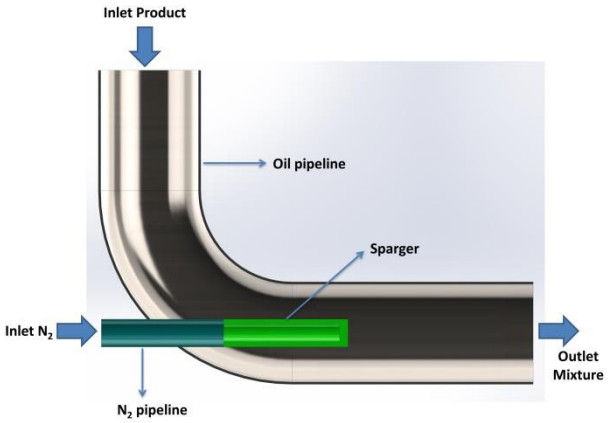

Figure 1: sparger's position inside vegetable oil pipeline

As can be noticed from Figure 1, the sparger is elbow mounted, in order to avoid the creation of a dead leg along the piping, from which could arise cleanability issues. The pipeline where vegetable oil flows is realized with commercial pipes having a nominal diameter of 80 mm (DN80, according to DIN standards), while the pipeline which carries gaseous N_2 to the sparger is realized with commercial pipes having a nominal diameter of 20 mm (DN20, according to DIN standards).

As previously explained, different geometrical configurations of the oil pipeline have been analyzed, in order to assess if a different geometry can influence N_2 distribution inside oil flow, and thus the removal of dissolved O_2. In particular, four configurations have been compared:

1. a configuration where the sparger is followed by a straight DN80 pipe;
2. a configuration where the sparger is followed by a Venturi-like pipe, with the Venturi throat having a diameter of 30 mm and the outlet section having a diameter of 50 mm;
3. a configurations where the sparger is followed by a Venturi-like pipe having some protuberances in the Venturi throat, to enhance the turbulence and, thus, the mixing between the gas and the vegetable oil (also in this case the diameter of the Venturi throat is equal to 30 mm and the diameter of the outlet section is equal to 50 mm);
4. a configuration where the sparger is followed by a Venturi-like pipe having some protuberances in the Venturi throat, but with the outlet section having a diameter equal to 80 mm.

The first configuration represents the standard system used in companies that adopt the sparging technology to preserve vegetable oil from deterioration.

In each one of the four analyzed configurations the distance between the top of the sparger and the outlet section is equal to 460 mm. The four configurations are highlighted in Figure 2.

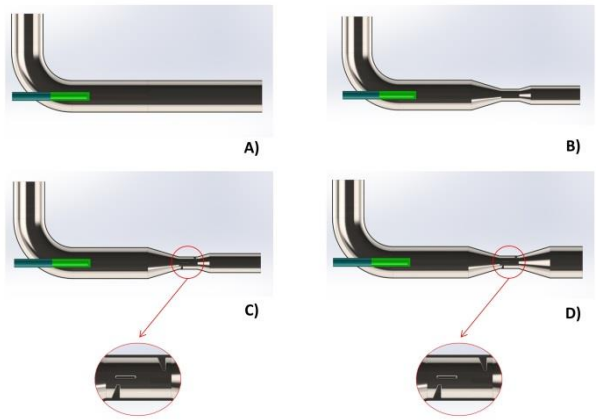

Figure 2: A) first configuration, B) second configuration, C) third configuration, D) fourth configuration

The tank considered in the simulation of the filling phase, instead, is a small capacity tank of 150 liters, made of stainless steel.

In particular, two version of the tank are adopted: in the first version the tank inlet section has a diameter of 80 mm (which will be coupled with sparging systems having a DN80 outlet), while in the second version it has a diameter of 50 mm (which will be coupled with sparging systems having a DN50 outlet). Connected to the inlet section there is a small-length pipe which

addresses the in-flow of vegetable oil towards the bottom of the tank. On the top of both versions, instead, there is a gas outlet, which allows the escape of the gas that accumulates above oil.

The following Figure 3 shows the two configurations of the tank adopted in the simulations.

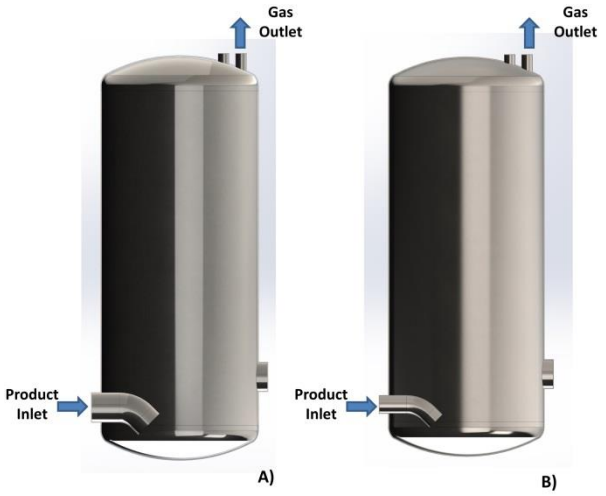

Figure 3: A) tank with DN80 inlet, B) tank with DN50 inlet

2.2. CFD Modelling

Considering the co-presence of a liquid phase (vegetable oil) and of two gaseous substances (N_2 and O_2) in this case a multi-phase simulation has to be set up.

Consequently, to set up the physics and solve the calculation, Ansys CFX version 16.1 has been used, because this software allows to simulate multi-phase flows. In fact, a 3D multi-phase simulation has been set up, considering a mixture of vegetable oil, N_2 and O_2.

In particular, in both simulations (sparger simulations and tank filling simulations) the "Homogeneous Model" has been adopted, in the first case because the fluids share the same velocity field, since the gases are entrained by the oil stream, and, in the second case, because it allows a better modeling of the free surface inside the tank, according to Ansys CFX Reference Guide.

In a multi-phase simulation, with the "Homogeneous Model" activated, the continuity equation becomes:

$$\frac{(r_\alpha \cdot \rho_\alpha)}{\partial t} + \nabla \cdot (r_\alpha \cdot \rho_\alpha \cdot \boldsymbol{U}) = \boldsymbol{S}_{MS_\alpha} + \sum_{\beta=1}^{N_p} \Gamma_{\alpha\beta} \qquad (1)$$

where:

- ρ_α is the density of phase α;
- r_α is the volume fraction of phase α;
- $\boldsymbol{U}$ is the vector of velocity $\boldsymbol{U}_{x,y,z}$, which is the same for all of the considered phases;
- $\boldsymbol{S}_{MS_\alpha}$ describes user specified mass sources;
- $\Gamma_{\alpha\beta}$ is the mass flow rate per unit volume from phase β to phase α. This terms only occurs if interphase mass transfer takes place, so in this case is equal to 0.

Instead, for the "Homogeneous Model", the momentum equation is given by:

$$\frac{(\rho \cdot \boldsymbol{U})}{\partial t} + \nabla \cdot \left(\rho \boldsymbol{U} \otimes \boldsymbol{U} - \mu(\nabla \boldsymbol{U} + (\nabla \boldsymbol{U})^T)\right) = \boldsymbol{S}_M - \nabla p \qquad (2)$$

where:

- $\rho = \sum_{\alpha=1}^{N_P} r_\alpha \rho_\alpha$ is the phase-averaged density;
- $\mu = \sum_{\alpha=1}^{N_P} r_\alpha \rho_\alpha$ is the phase-averaged dynamic viscosity;
- $\boldsymbol{S}_M$ is a term that describes a user specified momentum source.

Furthermore, is present a constraint which specifies that the volume fractions must sum up to unity in every instant and in every point of the fluid domain, meaning that the following equation:

$$\sum_{\alpha=1}^{N_p} r_\alpha = 1 \qquad (3)$$

has to be always respected.

With regard to energy exchanges, it has been considered that the analyzed processes are carried out at room temperature, with a negligible heat transfer between the fluid domain and the outside environment. Consequently, the isothermal model with a fixed temperature of 25°C has been set up.

Moreover, in the case of the tank filling simulations, to achieve a better modeling of the oil free surface, the "Standard Free Surface Model" has been adopted. In this case, if there are just two phases, the following equations is used for interfacial area density:

$$A_{\alpha\beta} = |\nabla r_\alpha| \qquad (4)$$

Finally, for both cases (sparger simulations and tank filling simulations) the *k-ε* turbulence model has been adopted, because it is suitable both for fluid flow inside in Venturi-like pipes (Guerra et al., 2012) and both for tank problems (Godderidge et al., 2009). The *k-ε* model is a two equations eddy viscosity turbulence model which is widely used to solve a large number of industrial problems (Blazek, 2015). The equation governing the k- *ε* model can be found in Ferziger and Peric (2002).

2.2.1. Mesh setting for the fluid domain

The fluid domains have been obtained starting from the 3D CAD models of the four sparger configurations and from the 3D CAD models of the two tank configurations by means of the CAD software SolidWorks (version 2014). Instead, the discretization of the fluid domains has been performed using the software Ansys Meshing version 16.1.

The grids were initially set by creating a uniform subdivision, and then thickened in the critical areas of the fluid domains.

In particular, considering the sparger configurations, a finer mesh was used near the inlets, near the outlet, near the walls and in the Venturi throat.

At the end of the operation, the unstructured grids obtained for the sparging simulations had, on average, a total of 680,000 nodes and 3,730,000 tetrahedrons each.

Figure 4 shows a section of the obtained volume meshes. In particular, Figure 4 A) shows the mesh for the first sparger configuration, Figure 4 B) shows a close-up of the mesh in the Venturi throat and Figure 4 C) shows a close-up of the mesh in the Venturi troath when the protuberances are present.

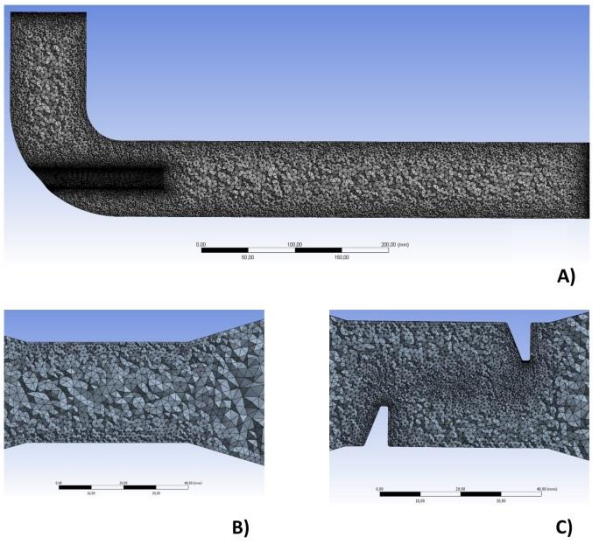

Figure 4: A) section of the volume mesh for first sparger configuration, B) close-up of the volume mesh in the Venturi throat, C) close-up of the volume mesh in the Venturi throat with protuberances

Also for the two tank configurations an unstructured grid has been adopted. Figure 5 shows a section of the volume mesh for both of the analyzed configurations.

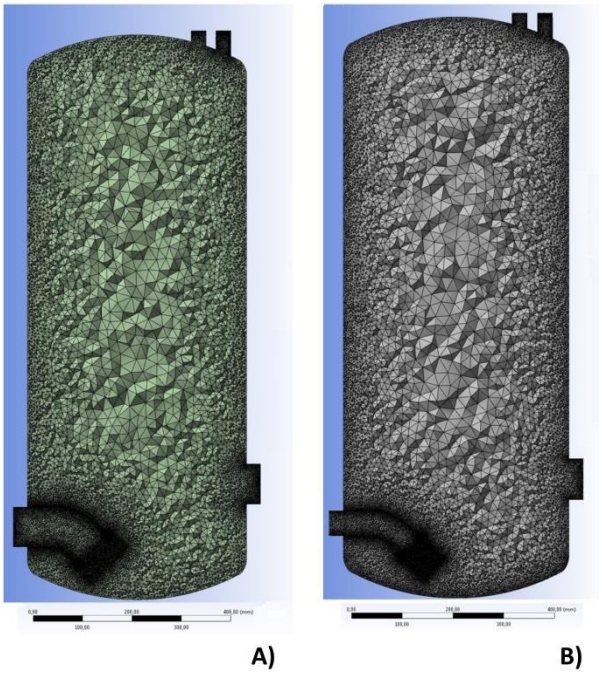

Figure 5: A) volume mesh for tank with DN80 inlet, B) volume mesh for tank with DN50 inlet

As can be noticed from Figure 5, in this case a finer mesh was adopted in correspondence of the gas outlet and in correspondence of the point where oil flows exits the inlet tube and enters the tank, which are the areas where the velocity gradients are expected to be higher.

An unstructured grid with about 1,000,000 nodes and 5,600,000 tetrahedrons was obtained for both tank configurations.

2.2.2. Simulation setting

Settings for sparger simulations

A 3D multi-phase simulation has been set up considering the fluid domain as composed by oil, N_2 and O_2.

N_2 and O_2 were considered as ideal gases and the values of the thermo-physical properties adopted for their characterization were the ones present by default in Ansys CFX materials database. Furthermore, since vegetable oil is not present in Ansys CFX materials library, it has been created using the settings showed in Table 1. In particular, the values adopted to define the thermo-physical properties of this substance are referred to Olive Oil characteristics at 25°C and atmospheric pressure.

Table 1: Olive Oil settings

Olive Oil Settings	
Thermodynamic State	Liquid
Density	916 $\frac{kg}{m^3}$
Molar Mass	276.72 $\frac{g}{mol}$
Specific Heat Capacity	2090 $\frac{J}{kg\,K}$
Specific Heat Type	Constant Pressure
Reference Temperature	25 °C
Reference Pressure	1 atm
Dyamic Viscosity	0.08 Pa·s
Thermal Conductivity	0.169 $\frac{w}{m\,K}$

Obviously, Olive Oil is not a pure substance but a mixture of chemical compounds (mostly fatty acids), so it is not possible to define in an exact way the molar mass for this element. Consequently, it has been obtained by calculating the weighted average of the molar masses of the oil main components.

Figure 6 shows the boundary conditions adopted for this set of simulations.

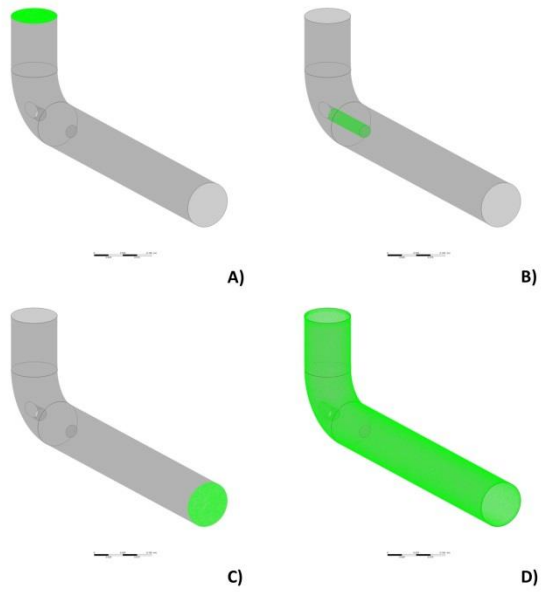

Figure 6: boundaries for sparging simulation: A) product inlet, B) N_2 inlet, C) outlet, D) wall

From Figure 6 B) can be noticed that the sparger has not been modeled as a porous domain but that the sparger's external walls have simply been set as a N_2 inlet. This has been done because we were not interested in modeling the N_2 pressure loss trough the sparger but only the achievable distribution of N_2 inside the oil stream. However, only the 70% of the inlet surface was considered as emanating N_2, and the generated gas bubbles have been considered with a diameter of 40 µm, in order to take account of the porosity and the average diameter of the sparger's pores.

The values set on the boundary conditions previously described are shown in Table2.

Table 2: boundary and initial conditions for original case

Buondary Conditions	
Product inlet	Mass Flow-Rate = 1.273 kg/s Oil volume fraction = 97.3 % O_2 volume fraction = 2.7 % N_2 volume fraction = 0
N_2 inlet	Mass Flow-Rate = 4.0e-4 kg/s Oil volume fraction = 0 O_2 volume fraction = 0 N_2 volume fraction = 100 %
Outlet	Relative pressure = 0,718
Wall	No Slip Wall Adiabatic
Initial Conditions	
Domain Composition	Oil volume fraction = 97.3 % O_2 volume fraction = 2.7% N_2 Volume fraction = 0
Velocity	0 m/s
T	25°C
p	1 bar

From the previous Table it can be noticed that, on the product inlet and in the initial domain composition, has been set an O_2 volume fraction equal to 2.7%. This has been done to consider that there could be a maximum of 36 mg/l of dissolved O_2 in vegetable oil (Parenti et al., 2007.). Instead, N_2 flow rate has been calculated considering that are necessary about 0.34 m^3 of N_2 in order to supersaturate 1 m^3 of oil, as reported by O'brien (2008).

The outlet pressure, instead, was chosen considering that on the outlet section there must be an adequate counter pressure to make sparging process effective.

The analysis was stationary, because product flow and N_2 flow have considered not time dependent.

Obviously the simulation and boundary conditions settings were the same for all of the analyzed sparger configurations.

Settings for tank filling simulations

Also in this case a 3D multi-phase simulation has been set up considering the fluid domain as composed by oil, N_2 and O_2.

As previously explained N_2 and O_2 were considered as ideal gases, while oil thermo-physical properties were created considering Olive Oil characteristics at 25°C and atmospheric pressure.

The boundary conditions adopted for these simulations are shown in Figure 7.

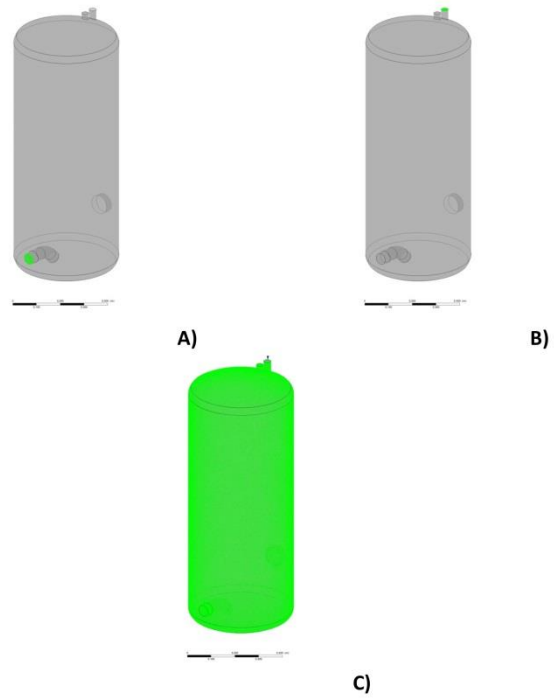

Figure 7: boundaries for tank filling simulation: A) tank inlet, B) tank gas outlet, C) wall

In this case on the tank inlet will be imported the results obtained on the outlet section at the end of the sparging process simulation. In particular will be imported the volume fractions and the flow velocity.

On the gas outlet atmospheric pressure, a N_2 volume fraction equal to 78.5% and a O_2 volume fraction equal to 21.5%, in order to reproduce air presence. Moreover, also in this case on the domain walls was set a no-slip adiabatic condition.

Finally, in this case, the analysis was carried out in transient mode, because to model the increase of product quantity inside the tank is necessary to consider the passing of time. In particular a total time of 110 s has been simulated, with a time-step of 0.05 s. The results were registered every 2.5 s. At 90 s the product in-flow has been interrupted, so to allow, in the last 20 s of the simulation, the diffusion of gas dissolved in vegetable oil through the product free surface. The time instant in which to stop the product in-flow has been chosen keeping in mind that 90 s is the time considered necessary, considering the flow rate, to have in the tank a product quantity such that the head space is equal to about the 20% of the volume of the tank itself. This has been done in accordance with a practical rule which says that the head space should be between 10% and 30% of the volume.

The conditions of the fluid domain at the beginning of the simulation are shown in Table 3.

Table 3: Tank filling simulation initial conditions

Initial Conditions	
Domain Composition	Oil volume fraction = 15% N_2 volume fraction = 85% O_2 volume fraction= 0
Velocity	0 m/s
T	25°C
p	1.7 bar

From Table 3 can be noticed that at the beginning of the simulation the tank is considered already partially filled with oil, which accumulates on its bottom, while the head space is filled with N_2. Consequently in analyzed case sparging and blanketing are applied simultaneously, to avoid the contact between the product and atmospheric O_2 during filling. An absolute pressure of 1.7 bar, instead, has been selected because it is the expected average absolute pressure on the outlet section on spargers configuration, considering the setting adopted for these analyses.

3. RESULTS AND DISCUSSION

3.1. CFD simulation of the sparging process

The first analyses that were performed have been the ones involving the four different configurations adopted for the sparging process. The simulations converged after about 500 iterations.

In this case the main analyzed result was the N_2 distribution on the outlet section of the systems. These results are summarized in Figure 8, which shows N_2 volume fraction for each one of the four analyzed configurations.

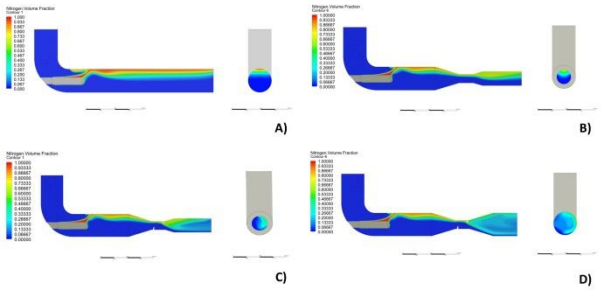

Figure 8: N_2 distribution inside sparging system: A) N_2 volume fraction in first configurations, B) N_2 volume fraction in second configuration C) N_2 volume fraction in third configuration, D) N_2 volume fraction in fourth configuration

It can be noticed that, in the first configuration (Figure 8 A), gaseous N_2 tends to stratify above vegetable oil and, consequently, N_2 distribution on the outlet section is not homogeneous. Also the second configuration (Figure 8 B)) is affected by this problem, although to an slightly smaller extent, thanks to the introduction of the Venturi. On the contrary, in the third and in the fourth configuration (Figure 8 C) and D)), the protuberances placed in the Venturi throat allow to achieve a better mixing between N_2 and the product in

the final part of the pipeline, thus obtaining a more homogeneous N_2 distribution on the outlet section.

Also a quantitative analysis of these results was performed, which is highlighted in Figure 9.

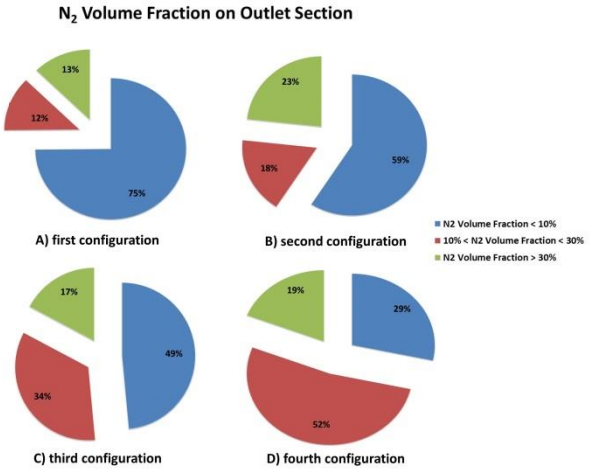

Figure 9: N_2 distribution on the outlet section of the sparging systems

As can be observed from the previous Figure, in the third and in the fourth configuration, the percentage of the outlet section area where N_2 volume fraction is lower than 10% is considerably lower than in the first two configurations. Consequently, we can say that the introduced changes improve the mixing between N_2 and the product. Then, the simulations of the tank filling phase will highlight if the realized changes have an impact also on the amount of the dissolved O_2 that can be removed.

Other analyzed results are the average absolute pressure and the average velocity on the outlet section, which are shown in Table 4.

Table 4: Average absolute pressure and average velocity on outlet section

	Configurations			
Variables	Conf. 1	Conf. 2	Conf. 3	Conf. 4
Average Absolute Pressure	1.73 bar	1.73 bar	1.73 bar	1.73 bar
Average Velocity	0.36 m/s	0.87 m/s	0.93 m/s	0.69 m/s

It may be noticed that the average absolute pressure on the outlet section is 1.73 bar, which confirms the correctness of the settings regarding the initial pressure for the simulations of the tank filling phase.

3.2. CFD simulations of tank filling

In this section are presented the results of the simulations of the tank filling phase. In particular three simulations have been carried out:

1) tank filling starting from the results obtained at end of the analysis of the first sparger configuration;
2) tank filling starting from the results obtained at the end of the analysis of the third sparger configuration;
3) tank filling starting from the results obtained at the end of the analysis of the fourth sparger configuration.

To carry out the simulations the results obtained on the spargers outlet section in terms of velocities and volume fractions were imported on tank inlet. A coupling between the second sparger configuration and the tank was not analyzed, because the N_2 distribution on the outlet section of the sparging system was deemed too similar to that obtainable with the first analyzed system.

In this case, the main analyzed result is evolution in time of the O_2 residual in oil. The graph in Figure 10 compares the O_2 residual for the three simulated configurations.

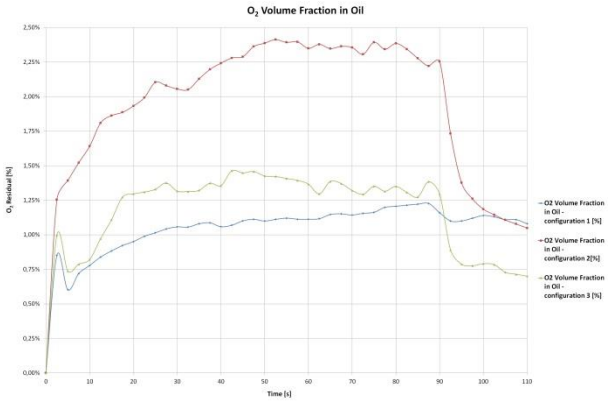

Figure 10: O_2 residual in oil for the three tank filling simulations

First of all, it can be noticed that, for all of the three analyzed configurations, O_2 residual in oil increases for the first 90 s, then, when the filling is stopped, the injected N_2 starts to spread through the product free surface, dragging O_2 along with itself and thus causing a rapid decrease of the residual, as expected. This trend is more pronounced for the second and the third configurations than in the first one.

It can be observed that the first configuration allows to reach a final O_2 residual in oil equal to 1.08%, starting from an initial average volume fraction of O_2 in oil, on the inlet section, equal to 2.4%. Moreover, in this case O_2 residual in oil during filling never reaches a value higher than 1.23% (at 87.5 s). This value is lower than the O_2 volume fraction on inlet section, consequently, in this case, seems that N_2 is pushing O_2 towards the outlet section also during the filling phase.

This phenomenon is confirmed also for the third analyzed configuration. In this case, the final O_2

residual is equal to 0.7% (also in this case starting from an initial average volume fraction of O_2 in oil, on the inlet section, equal to 2.4%) while, the maximum value reached by O_2 volume fraction in oil during filling, is equal to1.46%.

Instead, in the second configuration, the final O_2 residual in oil is equal to 1.04%, starting from a O_2 volume fraction on inlet of 2.4%. Moreover, the maximum value reached by O_2 volume fraction in oil during filling, is equal to 2.4%, showing how, in this case, injected N_2 is less effective in eliminating dissolved O_2 during filling. This could be related to the higher average velocity on tank inlet which, excluding the different N_2 distribution in oil stream, is the main difference between this configuration and the other two.

3.3. Discussion

The results described in section 3.2 are summarized in the following Table 5.

Table 5: O_2 residual after tank filling

	O_2 residual after tank filling			
	O_2 volume faction on inlet	Max O_2 volume fraction in Oil during filling	Final O_2 residual in Oil	% decrease of dissolved O_2
Sim. 1	2.40 %	1.23 %	1.08 %	55 %
Sim. 2	2.40 %	2.40 %	1.04 %	57 %
Sim. 3	2.40 %	1.46 %	0.70 %	71 %

Comparing the residuals highlighted in Table 5 we can say that simulation 2 (coupling between tank and third sparger configuration) and simulation 3 (coupling between tank and fourth sparger configuration) show better results than simulation 1. In particular, the best case seems to be simulation 3, which allows to reduce the amount of dissolved O_2 by 71%. Consequently, we can say that the sparging configuration and the N_2 distribution inside the oil stream have an important influence on the removal process of dissolved O_2.

Two points instead should be discussed: the trend in the decrease of O_2 volume fraction in oil when the filling stops (at 90 s) and the maximum O_2 volume fraction that is reached in oil during filling.

With respect to the first point, from Figure 10 can be seen that, when the filling stops, in simulation 2 and simulation 3 there is a drop in the amount of O_2 dissolved in oil. Instead, this does not happen in simulation 1, which shows only a small decrease. A possible explanation is in the amount of N_2 in the oil inside the tank. If we compare N_2 volume fraction in the tank at 92.5 s we can see that in the first simulation it is considerably lower than in the last two analyzed configurations, as highlighted in Figure 11. Consequently, also the quantity of O_2 pushed towards the outlet section is lower and thus, in simulation 1, is lower the drop in O_2 concentration.

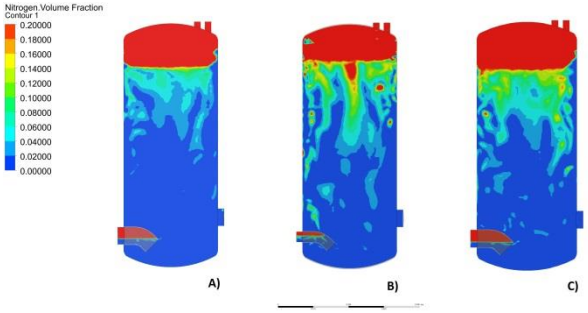

Figure 11: N_2 volume fraction in tank at 92.5 s: A) first tank simulation, B) second tank simulation, C) third tank simulation

Instead, considering the second point, again from Figure 10 it can be observed that, in simulation 2, during filling, the maximum concentration of O_2 that is reached in the bulk of oil is equal to 2.4%, while, in other simulations, is considerably lower (never higher than 1.46%). This means that, someway, in the second case N_2 cannot separate O_2 also during filling and that its action becomes significant only when the filling is stopped. This may be related to the higher fluid velocity. In this case, in fact, tank inlet has a DN50 section and, consequently, the average fluid velocity over the inlet is higher, as highlighted in in Table 4. This could lead to a very chaotic filling, which instead of favoring N_2 action partially hinders it. However, of fundamental importance will be a subsequent experimental phase, which will allow not only to test the model and modify it if necessary, but also to verify in laboratory the origin of these two behaviors.

4. CONCLUSIONS

The sparging process of vegetable oil with gaseous N_2 (or with another inert gas) is one of the most adopted techniques to preserve vegetable oil from spoilage. This technique consist in inject the inert gas directly in the oil stream by means of a porous sparger. Subsequently, the injected gas, during tank filling operation, diffuses trough the free surface on the product, and saturates tank head-space, preventing the contact between oil and atmospheric O_2, which is the major spoilage agent. In some cases sparging is used coupled with blanketing, which consists in saturating the tank inner volume with N_2, in order to create an inert environment. In this case sparging main goal is to separate the O_2 dissolved in the product, which could be present in quantity of 36 mg/l. In this case, when gaseous starts to diffuse through product's free surface, it drags along with itself parts of the dissolved O_2.

The objective of this work was to simulate various sparger configurations and the subsequent tank filling operation, to assess if the sparger geometry could affect the N_2 distribution inside the oil stream and, consequently, the O_2 removal process. In particular four different configurations were modeled:

1. a configuration where the sparger is followed by a straight DN80 pipe;
2. a configuration where the sparger is followed by a Venturi-like pipe, with the Venturi throat having a diameter of 30 mm and the outlet section having a diameter of 50 mm;
3. a configurations where the sparger is followed by a Venturi-like pipe having some protuberances in the Venturi throat, to enhance the turbulence and, thus, the mixing between the gas and the vegetable oil (also in this case the diameter of the Venturi throat is equal to 30 mm and the diameter of the outlet section is equal to 50 mm);
4. a configuration where the sparger is followed by a Venturi-like pipe having some protuberances in the Venturi throat, but with the outlet section having a diameter equal to 80 mm.

The first configuration represents the standard system used in companies that adopt the sparging technology to preserve vegetable oil from deterioration.

Configurations 3 and 4 allowed to obtain a more homogeneous N_2 distribution on the system outlet section and, consequently, they were coupled with the tank, to evaluate also the filling operation and the effectiveness of the O_2 removal process, in order to compare them with the original configuration.

At the end of these sets of simulations, has been verified that both configurations are more effective in removing the dissolved O_2 than the original one. In particular, the fourth sparger configuration was identified as the best case, since it allows to remove the 71% of the dissolved O_2, compared to the 55% obtained with the original configuration. This work, consequently, proved that the sparging system geometry and that the N_2 distribution inside the oil stream are very important to obtain an effective removal of dissolved O_2. In particular, simulations have shown that, with changes having a limited cost, is possible to increase the effectiveness of the removal process by 77%.

Points to be addressed are the trend in the O_2 residual in oil when the filling stops, which is different when adopting the original sparging system, and the fact that in one case there is a small accumulation of O_2 in the tank during filling.

Future researches should focus on the execution of an experimental phase, in order to validate the simulations described in this paper and to observe, in a laboratory, the origin of the two described unexpected behaviors.

Moreover, simulations of the described systems in a vertical position should be carried out, since, frequently, the adopted sparging solution is used also in this way.

REFERENCES

ANSYS CFX-solver modeling guide, release 16.1. ANSYS, Inc. Southpointe 2600 ANSYS Drive, 2015.

ANSYS CFX-solver theory guide, release 16.1. ANSYS, Inc. Southpointe 2600 ANSYS Drive, 2015.

Blazek, J., 2015. Computational fluid dynamics: principles and applications. Butterworth-Heinemann.

Bottani E, Ferretti G, Manfredi M, Vignali G. Modeling and thermo-fluid dynamic simulation of a fresh pasta pasteurization process. International Journal of Food Engineering, 9:327–39.

Choe, E., Min, D. B., 2006. Mechanisms and factors for edible oil oxidation. Comprehensive reviews in food science and food safety, 5(4), 169-186.

Ferziger JH, Peric M., 2002. Computational methods for fluid dynamics. Axel-Springer Verlag.

Godderidge, B., Turnock, S., Tan, M., Earl, C., 2009. An investigation of multiphase CFD modelling of a lateral sloshing tank. Computers & Fluids,38(2), 183-193.

Guerra, V. G., Béttega, R., Gonçalves, J. A., Coury, J. R., 2012. Pressure drop and liquid distribution in a venturi scrubber: experimental data and CFD simulation. Industrial & Engineering Chemistry Research, 51(23), 8049-8060.

Gunstone, F. (Ed.)., 2011. Vegetable oils in food technology: composition, properties and uses. John Wiley & Sons.

Manfredi, M., Vignali, G. 2015 Comparative Life Cycle Assessment of hot filling and aseptic packaging systems used for beverages. Journal of Food Engineering, 147, pp. 39-48.

Masella, P., Parenti, A., Spugnoli, P., Calamai, L., 2010. Nitrogen stripping to remove dissolved oxygen from extra virgin olive oil. European Journal of Lipid Science and Technology, 112(12), 1389-1392.

Mosna, D., Vignali, G. 2015. Three-dimensional cfd simulation of a "steam water spray" retort process for food vegetable products. International Journal of Food Engineering, 11 (6), pp. 715-729.

O'brien, R. D., 2008. Fats and oils: formulating and processing for applications. CRC press.

Parenti, A., Spugnoli, P., Masella, P., & Calamai, L., 2007. Influence of the extraction process on dissolved oxygen in olive oil. European journal of lipid science and technology, 109(12), 1180-1185.

Shahidi, F., 2005. Bailey's Industrial Oil and Fat Products, 6 Volume Set (Vol. 1).

Shahidi, F., 2005. Bailey's Industrial Oil and Fat Products, 6 Volume Set (Vol. 5).

Spanu, S., Vignali, G. 2015. CFD analysis of coffee packaging in capsules using gas flushing modified atmosphere packaging. International Food Operations and Processing Simulation Workshop, FoodOPS 2015, pp. 1-8.

Spanu, S., Vignali, G., in press. Modelling and Multi-objective Optimisation of the VHP Pouch Packaging Sterilisation Process. International Journal of Food Engineering, DOI: 10.1515/ijfe-2015-0061

AUTHORS BIOGRAPHY

Filippo FERRARI is a recent graduate at the University of Parma. After taking the bachelor degree in engineering management in February 2014, in July 2016 he has achieved a master degree in Mechanical Engineering for the Food Industry at the same University. His main fields of interest concern food process modelling and simulation.

Simone SPANU is a scholarship holder at CERIT research center at the University of Parma. In March 2014 he has achieved a master degree in Mechanical Engineering for the Food Industry at the same university. His main fields of research concern food process modelling and simulation, with a particular focus on the CFD simulation for the advanced design of food and beverage processing plants.

Giuseppe VIGNALI is an Associate Professor at University of Parma. He graduated in 2004 in Mechanical Engineering at the University of Parma. In 2009, he received his PhD in Industrial Engineering at the same university, related to the analysis and optimization of food processes. Since August 2007, he worked as a Lecturer at the Department of Industrial Engineering of the University of Parma. His research activities concern food processing and packaging issues and safety/security of industrial plant. Results of his studies related to the above topics have been published in more than 70 scientific papers, some of which appear both in national and international journals, as well in national and international conferences.